MEASUREMENTS OF PLASMA PARAMETERS NEAR RESONANCE ZONES AND PERIPHERAL REGIONS IN ECRIS

W. Kubo[†], S. Harisaki, I. Owada, K. Sato, K. Tsuda, and Y. Kato,
Division of Electrical, Electronic and Infocommunications Engineering, Graduate School of
Engineering, Osaka University, 2-1 Yamada-oka, Suita-shi, Osaka 565-0871, Japan

Abstract

Electron cyclotron resonance ion source (ECRIS) has a wide range of application, *e.g.*, cancer treatment and material synthesis. We have constructed the ECRIS which can provide various ion species and investigated how to produce multicharged ions efficiently in Osaka University. In recent years, we have focused on waves propagations in plasma and conducted the upper-hybrid resonance (UHR) experiments. The second microwaves whose frequencies are much higher than fundamental ECR's one are superimposed to the ECR plasma. We have also conducted experiments heating by the coaxial semi-dipole antenna with the aim of enhancing the right-hand polarization (RHP) wave, which contributes to ECR.

We measure simultaneously plasma parameters in those regions by two Langmuir probe inserted into each location under the same operation condition. These probes are set at the upperstream and the downstream of the ECR zone. We measure the electron energy distribution function (EEDF) and the ion saturation current I_{is} in the two regions. We presume RHP waves propagation near the ECR zone by comparing measurements results and the accessibility of the RHP wave in the ECRIS. The accessibility is estimated from the $\boldsymbol{B}$ profiles by the calculation and the n_e profiles obtained by the fitting with the past measurements. In near future, we optimize the coaxial semi-dipole antenna in order to optimize the ECR efficiency by the 2.45 GHz microwave.

INTRODUCTION

Ion sources based on electron cyclotron resonance (ECRIS) have a wide range of applications, *e.g.*, cancer treatment and material synthesis [1, 2]. We have constructed the ECRIS, which can provide various ion species efficiently for those various applications. We have investigated how to produce multicharged ions efficiently in Osaka University [3-6]. We have focused on waves propagations in ECR plasma and conducted the upper-hybrid resonance (UHR) experiments. The second microwave (4-6 GHz) whose frequencies are much higher than fundamental ECR's one (2.45 GHz) are superimposed to ECR plasma as extraordinary (X) mode and got evidences for occurrence of UHR in the experiments [3-5]. We installed coaxial semi-dipole antenna, which is the new type antenna on the mirror end along the geometrical axis of the vacuum chamber. We compared ion beams extracted from the ECRIS with the new antenna and that with conventional one which is the rod antenna installed on the side wall of the vacuum chamber. We obtain the experimental results

---

† w.kubo@nf.eie.eng.osaka-u.ac.jp

that the coaxial semi-dipole antenna contributes to stable increase of the multicharged ion beams at high power [7].

Multicharged ion beams have been improved using various methods, *e.g.,* increasing of the magnetic field strength and the microwave frequency, using the DC biased plate-tuner, mixing low z gases, and heating by multiple frequencies. However the position of microwave launching has been empirically determined on conventional ECRIS. There is still room for improvement with the respect to more efficient excitation of the RHP wave propagation. The objective of this research is the estimation of the propagation of the RHP wave near the ECR zone, and in the opposite peripheral region beyond it. We measure simultaneously plasma parameters in those regions by two Langmuir probe inserted into each location under the same operation condition. We can measure plasma parameters, *i.e.,* the electron density n_e, the electron temperature T_e, the I_{is}, and the EEDF. We measure EEDF's and I_{is}'s in the upperstream and downstream regions near the ECR zone. We observe that I_{is}'s and tails of EEDF's measured on the side closer to the microwave launching are higher than those on the other side. These results are consistent with the propagation theory of the RHP wave in the ECR plasma. We compare extracted ion beams by launching microwaves from the coaxial semi-dipole antenna and the rod antenna.

BRIEF THEORICAL BACKGROUND AND EXPERIMENTAL APPARATUS

The RHP waves which give rise to ECR are transverse electric (TE) mode and propagate in the direction parallel to magnetic fields. On the basis of the RHP wave dispersion relationship for the case of no collisions and infinite mass ions, the RHP wave refraction index N_r can be written using the electron plasma frequency f_{pe} and the electron cyclotron frequency f_{ce} as following:

$$N_r{}^2 = \left(v_\varphi{}^2 \big/ c^2 \right)^{-1} = 1 - \frac{f_{pe}{}^2}{f(f - f_{ce})} \qquad (1)$$

where f is the frequency of incident microwave (RHP wave), v_φ is the phase velocity of the RHP wave, and c is the velocity of light.

Figure 1 shows the typical dispersion relationship of the RHP wave. The vertical and horizontal axes show $v_\varphi{}^2/c^2$ and f respectively. There is three regions A ($f < f_{ce}$), B ($f_{ce} < f < f_R$), and C ($f_R < f$) where f_R is the R-cutoff frequency which is the cutoff of the RHP wave ($N_r \to 0$). A and C regions are propagation regions of the RHP wave ($v_\varphi{}^2 > 0$) and B region is the non-propagation region ($v_\varphi{}^2 < 0$). The f_{ce} depends on the magnetic field

strength B and the f_R depends on B and the n_e. The microwave frequency launched to the vacuum chamber (2.45 GHz) relatively move between the three regions (A, B and C) in the dispersion relationship with the change of the f_{ce} and the f_R.
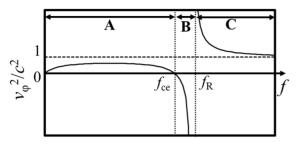

Figure 1: The typical dispersion relationship of RHP waves.

Figure 2(a) and 3(a) shows a schematic drawing of the ECRIS in Osaka Univ. It consists of a cylindrical vacuum chamber (160 mm in inner diameter and 1074 mm in Fig. 2(a)/1054 mm in Fig. 3(b) in length) with several ports at the top and the side wall. We use the cartesian coordinate system (x, y, z) with the origin located at the center of the chamber. The magnetic configuration of the ECRIS is formed by mirror coils (Coil A and B), an additional coil (Coil C), and permanent octupole magnets. Currents of three coils are defined as I_A, I_B, and I_C, respectively. Normally, the I_A and the I_B are 150 A, occasionally 170 A, and the I_C is optimized within ±20 A. The ECR zone is formed in the center of the chamber and is controllable by adjusting the I_C. 2.45 GHz microwaves are generated by the magnetron (incident microwave power 1.3 kW at the maximum) and are introduced into the vacuum chamber of the ECRIS thorough the coaxial window. We launch them from coaxial semi-dipole antenna z=-448 mm, in Fig. 2(b) or the rod antenna z=-175 mm, in Fig. 2(c) installed on the side wall of the vacuum chamber. The coaxial semi-dipole antenna is installed along the geometrical axis of the vacuum chamber in consideration of RHP wave propagation which is parallel to the B field [7-9]. The shape of the coaxial semi-dipole antenna is L-shape at the tip because we aim to exciting RHP waves by enhancing TE mode [7-9] in Fig. 2(b). The aluminum plate tuner (120 mm in diameter and 2 mm in thickness) is inserted behind the semi-dipole antenna. It is movable horizontally from z=-498 mm to z=-468 mm.

The operating gas is Ar and operating pressures are 10^{-4}~10^{-3}Pa. Langmuir probes LP1 (z=-175 mm) and LP2 (z=175 mm) and L-shape probe (z=364 mm) are inserted from the side port of the vacuum chamber and the plasma electrode in the case I in Fig. 2(a) and II in Fig. 3(a) respectively. LP1, 2 and L-shape probe consist of cylindrical Mo wires of 0.5 mm in diameter and 10 mm for LP1 and LP2 and 15 mm for L-shape probe in length in Fig. 2(d) and in Fig. 3(b). They are movable within x=0-50 mm for LP1 and LP2, and movable in the direction of the rotation for L-shape probe. We can estimate the plasma parameters, $e.g.$, the EEDF, the I_{is} (measured by applying -45V to probes), the n_e, and the T_e. Ion beam extraction electrodes
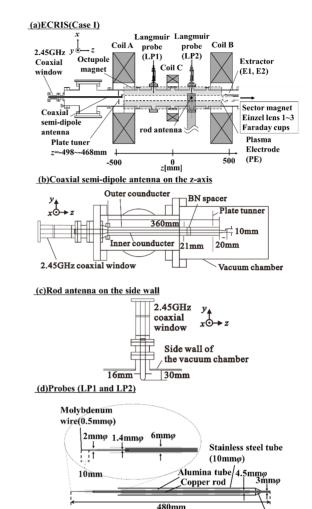

Figure 2: Schematic drawing of ECRIS (Case I) (a). Coaxial semi-dipole antenna installed on the z-axis (b). Rod antenna installed on the side wall of the vacuum chamber (c). Probes inserted from the side port (LP1 and LP2) (d).
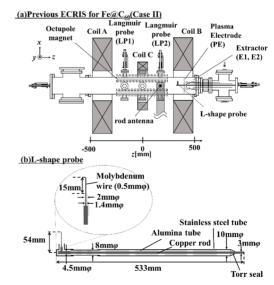

Figure 3: Schematic drawing of previous ECRIS for Fe@C_{60} (Case II) (a). L-shape probe inserted from the extractor (b).

consist of the plasma electrode (PE), the mid-electrode (E1), and the extractor electrode (E2) in Fig. 1(a). Extracted ion beams are focused by the einzel lens and analyzed by a sector magnet. Ion beam currents are measured by several Faraday cups. We can obtain the charge state distribution (CSD) of the extracted ion beam.

Figure 4 shows the typical accessibility condition in the x-z plane of the vacuum chamber estimated from the past measurements of n_e profiles and calculated B. Black and red lines represent the ECR and the R-cutoff regions respectively. It represents the location of the coaxial semi-dipole antenna, the rod antenna, and measurement regions of the LP1 and LP2. There is the B region, which is non-propagation region between the coaxial semi-dipole antenna and the rod antenna. It is considered that the RHP wave launched from each antenna difficult to reach the opposite region beyond the ECR zone. We consider that RHP waves from each antenna produce ECR more efficiently on the closer side with respect to the antenna than on the other side from the point of the accessibility condition. We measure and compare the plasma parameter I_{is} and EEDF in the two regions.
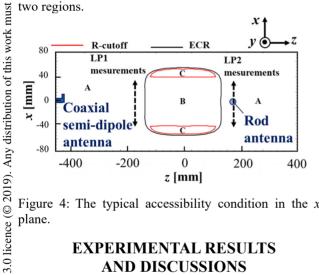

Figure 4: The typical accessibility condition in the x-z plane.

EXPERIMENTAL RESULTS AND DISCUSSIONS

Comparison of the I_{is}' Measured by LP1 and LP2 in the Case of the Microwave Launching by Each Antenna

Figure 5 shows comparison of the I_{is}'s profiles in the x direction measured by LP1 and LP2 in the case of the microwave launching by the coaxial semi-dipole antenna (a) and the rod antenna (b) under conditions which are I_c's are 11 and 15 A respectively. Vertical and horizontal axes are I_{is} and measurement positions x respectively. Red and blue plots represent measurement results of LP1 and LP2. In the case of the coaxial semi-dipole antenna, I_{is}'s measured by LP1 are higher than those by LP2. On the other hand, I_{is}'s measured by LP2 are higher than those by LP1 especially in the center of the vacuum chamber in the case of the rod antenna. These results indicate that the ECR on the side closer to the antenna is more efficient than the other side. This is consistent with propagation theory of RHP waves that they cannot pass through the B region above already mentions.
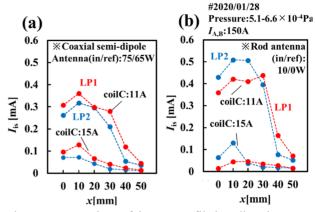
TUWZO01

Figure 5: comparison of the I_{is}'s profile in x direction measured by LP1 and LP2 in the case of the microwave launching by the coaxial semi-dipole antenna (a) and the rod antenna (b).

Comparison of the EEDF's Measured at z=-175 and 75 mm in ECRIS

Figure 6 shows comparison of the EEDF's measured by LP1 and LP2 at the x=0 in the case of the microwave launching by the coaxial semi-dipole antenna (a) and the rod antenna (b). Red and blue plots represent measurement results of LP1 and LP2. In both cases of microwave launching by each antenna, EEDF's measured on the side closer to each antenna have higher tail than the other side. We can calculate the effective electron energy T_{eff} from EEDF's. In the case of the coaxial semi-dipole antenna, T_{eff}'s are 12.9 eV (LP1) and 12.7 eV (LP2). In the case of the rod antenna, T_{eff}'s are 11.0 eV (LP1) and 9.72 eV (LP2). We observe that the EEDF measurement results indicate same tendencies as I_{is}, which are consistent with the propagation theory of RHP waves.
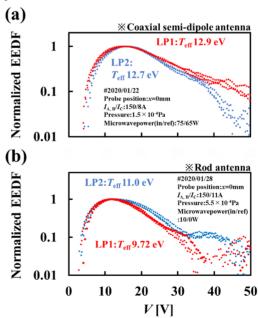

Figure 6: Comparison of the EEDF's measured by LP1 and LP2 at the x=0 in the case of the microwave launching by the coaxial semi-dipole antenna (a) and the rod antenna (b).

24th Int. Workshop on ECR Ion Sources
ECRIS2020, East Lansing, MI, USA
JACoW Publishing
ISBN: 978-3-95450-226-4
ISSN: 2222-5692
doi:10.18429/JACoW-ECRIS2020-TUWZ001

Typical CSD's of Ion Beams Extracted from Plasmas Produced by Each Antenna at Low and High Power

Figure 7 shows typical CSD of the ion beams extracted from Ar plasmas produced by each antenna at the low power 100W (a) and the high power 280-300W (b). The black and red plots represent the case of the coaxial semi-dipole antenna and the rod antenna respectively. At the low power in Fig. 7(a), the currents of multicharged ions ($Ar^{4\sim7+}$) are higher in the case of the microwave launching by the rod antenna than that by the coaxial semi-dipole antenna. We estimate that this tendency is caused by the location of the rod antenna, which is downstream with the respect to the ECR zone and on the side closer to the extractor. At the high power in Fig. 7(b), multicharged ion currents become unstably and start to decrease in the case of the rod antenna [7]. On the contrary, they continue to increase stably in the case of the coaxial semi-dipole antenna. This is because setting the antenna along the z-axis is suitable to the RHP wave propagation [7].
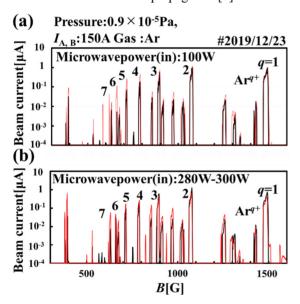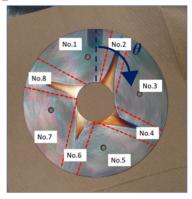

Figure 7: Typical CSD of the ion beams extracted from Ar plasmas produced by two probes at the low power 100W (a) and the high power 280-300W (b).
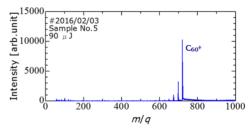
Plasma Parameters Measured Near the PE-plate by the L-shape Langmuir probe in ECRIS

Figure 8(a) shows PE-plate after experiments of synthesising Fe@C_{60}[6] in the previous ECRIS in Fig. 3(a). We can confirm the pattern of the plasma confined by the octupole. We divide it into 8 regions (No. 1~8). We analysis the two regions (No. 5 and 6) by the time of flight mass spectrometry (TOFMS). We observe the spectrum of C_{60}^{+} in the No. 5 in Fig. 8(b) and materials which have same m/q as Fe@C_{60} and Fe@C_{58} in the No. 6 in Fig. 8(c).

(a)PE-plate

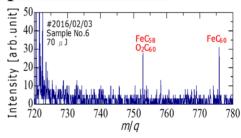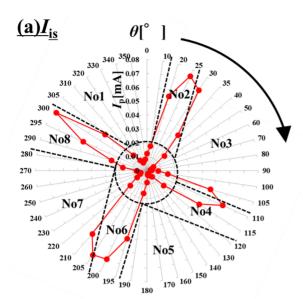### (b)Spectrum in No. 5

(c)Spectrum in No. 6

Figure 8: PE-plate after experiments of synthesising Fe@C_{60} (a). Spectrum of the TOFMS analysis in the No. 5 region (b). That in the No. 6 region (c).

Figure 9 shows measurement results by rotating the L-shape probe in Fig. 3(b). We measure the dependence of the I_{is} on the angle θ in Fig. 9(a). The I_{is} peak in the even number regions (No. 2, 4, 6, 8). We measure EEDF's at $\theta =205°$ in the No. 6 and those at $\theta =190°$ in the boundary region between No. 5 and No. 6 in Fig. 9(b). They are represented by red and black plots respectively. It is observed that the EEDF at $\theta =205°$ has higher tail than that at $\theta =205°$. There are higher energy electrons in the No. 6 where productions of Fe@C_{60} and Fe@C_{58} is suggested.
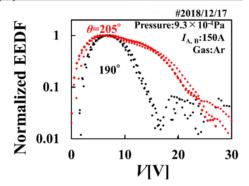
Figure 9: I_{is} measured by L-shape probe (a). EEDF's measured at the θ =205° and 190° (b).

REFERENCES

[1] A. Kitagawa *et al.*, "Status of Ion Sources at HIMAC", in *Proc. 19th Int. Workshop on ECR Ion Sources (ECRIS'10)*, Grenoble, France, Aug. 2010, paper MOCOBK03, pp. 20-22.

[2] T. Uchida, H. Minezaki, K. Tanaka, M. Muramatsu, T. Asaji, Y. Kato, A. Kitagawa, S. Biri, and Y. Yoshida, "Bio-Nano EC-RIS: An electron cyclotron resonance ion source for new materials production", *Rev. Sci. Instrum.*, vol. 81, p. 02A306, 2010.
doi.org/10.1063/1.3258027

[3] Y. Kato, T. Nishiokada, K. Hamada, K. Onishi, T. Takeda, K. Okumura, T. Omori, W. Kubo, M. Ishihara, and S. Harisaki, "Upper hybrid resonance heating experiments by X-mode microwaves on electron cyclotron resonance ion source', *Rev. Sci. Instrum.*, vol. 91, p. 013315, 2020.

[4] T. Nishiokada, T. Nagaya, S. Hagino, T. Otsuka, M. Masayuki, F. Sato, A. Kitagawa, and Y. Kato, "Experimental results of superimposing 9.9 GHz extraordinary mode microwaves on 2.45 GHz ECRIS plasma", *Rev. Sci. Instrum.*, vol. 87, p. 02A714, 2016.
doi.org/10.1063/1.4934212

[5] Y. Kato, T. Nishiokada, T. Nagaya, S. Hagino, T. Otsuka, T. Watanabe, Y. Tsuda, K. Hamada, K. Onishi, T. Takeda and T. Asaji, "Preliminary results of 4.0-6.0 GHz extraordinary mode experiments on 2.45 GHz ECRIS", *AIP Conference Proceedings*, vol. 2011, no. 1, p. 020005, 2018.
doi.org/10.1063/1.5053247

[6] Y. Kato, T. Nagaya, T. Nishiokada, S. Hagino, T. Otsuka, T. Watanabe, Y. Tsuda, K. Onishi, K. Hamada, T. Takeda, T. Uchida, M Muramatsu, A. Kitagawa and T. Asaji", Production of nitrogen-fullerene compound ion beams on tandem-type electron cyclotron resonance ion source", *AIP Conference Proceedings*, vol. 2011, p. 090013, 2018.
doi.org/10.1063/1.5053394

[7] W. Kubo, K. Hamada, K. Onishi, T. Takeda, K. Okumura, T. Omori, M. Ishihara, S. Harisaki, and Y. Kato, "Coaxial semi-dipole antenna microwave feeding on electron cyclotron resonance multicharged ion source", *Rev. Sci. Instrum.*, vol. 91, p. 023317, 2020.
doi.org/10.1063/1.5128576

[8] Francis F. Chen, "*Introduction to Plasma Physics*", New York, Plenum Press, 1974.

[9] Michael A. Lieberman and Allan J. Lichtnberg, in "*Principle of Plasma Discharges and Materials Processing*", New York, NY, USA: Wiley, 1994.